We are IntechOpen,
the world's leading publisher of
Open Access books
Built by scientists, for scientists

6,900
Open access books available

186,000
International authors and editors

200M
Downloads

Our authors are among the

154
Countries delivered to

TOP 1%
most cited scientists

12.2%
Contributors from top 500 universities

CLARIVATE ANALYTICS
BOOK CITATION INDEX
INDEXED

WEB OF SCIENCE™

Selection of our books indexed in the Book Citation Index
in Web of Science™ Core Collection (BKCI)

Interested in publishing with us?
Contact book.department@intechopen.com

Numbers displayed above are based on latest data collected.
For more information visit www.intechopen.com

Fracture Variation of Welded Joints at Various Temperatures in Liquid-Phase-Pulse-Impact Diffusion Welding of Particle Reinforcement Aluminum Matrix Composites

Kelvii Wei Guo

Abstract

The fracture variation of liquid-phase-pulse-impact diffusion welding (LPPIDW) welded joints of aluminum matrix composites (ACMs: $SiC_p/A356$, $SiC_p/6061Al$, and $Al_2O_{3p}/6061Al$) was investigated. Results show that under the effect of pulse-impact (i) initial pernicious contact state of reinforcement particles changes from reinforcement (SiC, Al_2O_3)/reinforcement (SiC, Al_2O_3) to reinforcement (SiC, Al_2O_3)/matrix/reinforcement (SiC, Al_2O_3) and (ii) the fracture of welded joints with optimal processing parameters is the dimple fracture. Meanwhile, scanning electron microscope (SEM) of the fracture surface shows some reinforcement particles (SiC, Al_2O_3) in the dimples. Moreover, the slight reaction occurs at the interfaces of SiCp/6061Al, which is propitious to improve the property of welded joints because of the release of internal stress caused by the hetero-matches between the reinforcements and matrix. Consequently, aluminum matrix composites ($SiC_p/A356$, $SiC_p/6061Al$, and $Al_2O_{3p}/6061Al$) were welded successfully.

Keywords: aluminum matrix composite, fracture, fractography, particle reinforcement, pulse-impact, diffusion welding

1. Introduction

Aluminum matrix composites (AMCs) have a wide application in the fields of aerospace, automobile, structural components, heat-resistant-wearable parts in engines, and so on due to their high specific strength, rigidity, wear resistance, corrosion, and good dimensional stability [1–5]. The reinforcements in AMCs may be either in the form of particulates or as short fibers, whiskers, etc. [5, 6]. These discontinuous natures create several problems to their joining techniques for acquiring their high strength and good quality welded joints.

The high specific strength, good wearability, and corrosion resistance of aluminum matrix composites (AMCs) attract substantial industrial applications. Typically, AMCs are currently used widely in automobile and aerospace industries, structural components, heat-resistant-wearable parts in engines, etc. [7–10]. The particles of reinforcement elements in AMCs may be either in the form of particulates or as short fibers, whiskers, and so forth [10, 11]. These discontinuous natures create several problems to their joining techniques for acquiring their high strength and good quality welded joints. Typical quality problems of those welding techniques currently available for joining AMCs [12–20] are as elaborated below.

(1) The distribution of particulate reinforcements in the weld.

As properties of welded joints are usually influenced directly by the distribution of particulate reinforcements in the weld, their uniform distribution in the weld is likely to give tensile strength higher than 70–80% of the parent AMCs. Conglomeration distribution or the absence (viz., no reinforcement zone) of the particulate reinforcements in the weld generally degrades markedly the joint properties and subsequently resulted in the failure of welding.

(2) The interface between the particulate reinforcements and aluminum matrix.

High welding temperature in the fusion welding methods (typically TIG, laser welding, electron beam, etc.) is likely to yield pernicious Al_4C_3 phase in the interface. Long welding time (e.g., several days in certain occasions) in the solid-state welding methods (such as diffusion welding) normally leads to (i) low efficiency and (ii) formation of harmful and brittle intermetallic compounds in the interface.

To alleviate these problems incurred by the available welding processes for welding AMCs, a liquid-phase-pulse-impact diffusion welding (LPPIDW) technique has been developed [21–23]. This work aims at providing some specific studies that influence the pulse-impact on the fractography variation of welded joints. Analysis by means of scanning electron microscope (SEM), transmission electron microscope (TEM), and X-ray diffraction (XRD) allows the micro-viewpoint of the effect of pulse-impact on LPPIDW to be explored in more detail. Also, temperature distribution in heated sample also calculates.

# 2. Experimental material and procedure

2.1. Material

Stir-cast SiC_p/A356, P/M SiC_p/6061Al, and Al_2O_{3p}/6061Al aluminum matrix composite, reinforced with 20%, 15% volume fraction SiC, Al_2O_3 particulate of 12 μm, 5 μm mean size, were illustrated in **Figure 1**.

2.2. Experimental procedure

The quench-hardened layer and oxides induced by wire-cut process, on the surfaces of aluminum matrix composite specimens, were removed by polishing with 400 # grinding paper carefully. The polished specimens were then properly cleaned by acetone and pure ethyl alcohol so as to remove any contaminants off its surfaces. A DSI Gleeble®-1500D

SiC$_p$/A356
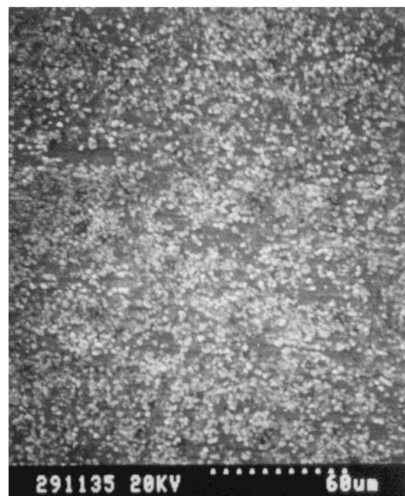
SiC$_p$/6061Al
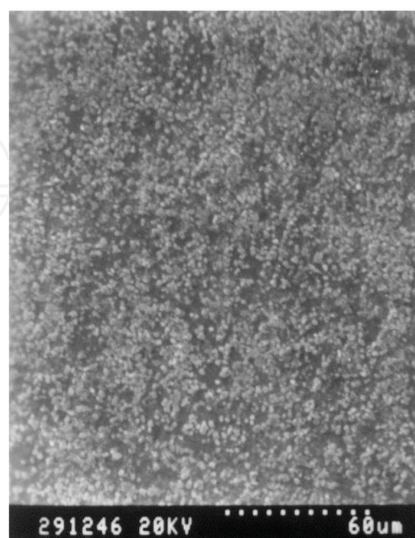
Al$_2$O$_{3p}$/6061Al

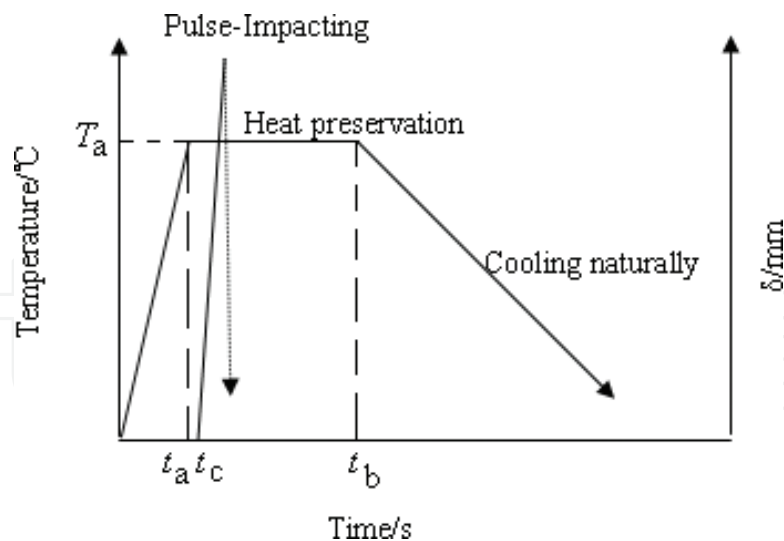**Figure 1.** Microstructure of aluminum matrix composites.

Figure 2. Schematic diagram of liquid-phase-pulse-impact diffusion welding.

thermal/mechanical simulator with a 4×10^{-1} Pa vacuum chamber was subsequently used to perform the welding.

The microstructures and the interface between the reinforcement particle and the matrix of the welded joints were analyzed by SEM, TEM, and XRD.

2.3. Operation of LPPIDW

Figure 2 shows a typical temperature and welding time cycle of a LPPIDW. It basically involves with (i) an initially rapid increase of weld specimens, within a time of t_a, to an optimal temperature T_a at which heat was preserved constantly at T_a for a period of (t_b-t_a); (ii) at time t_c, a quick application of pulse-impact to compress the welding specimens to accomplish an anticipated deformation δ within 10^{-4}–10^{-2} s, whilst the heat preservation was still maintained at the operational temperature T_a; and (iii) a period of natural cooling to room temperature after time t_b.

3. Results and discussion

3.1. Temperature distribution calculation in heated sample

The schematic diagram of temperature distribution in heated sample is shown in **Figure 3**, where L is the length of sample between two holders.

T_0 is the initial temperature. When the sample is heated, the heat transfer at the distance of x in Δt is

$$Q = -\alpha A \frac{\partial T}{\partial x} \Delta t \tag{1}$$

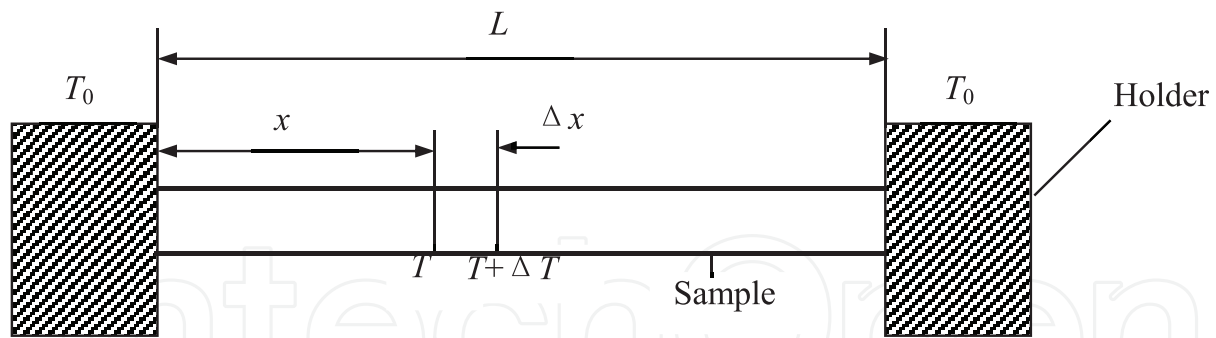where α is the coefficient of conduction and A is the cross-sectional area.

Figure 3. Schematic diagram of temperature distribution in heated sample.

At the same time, the heat transfer at the distance of $(x + \Delta x)$ is

$$Q + \Delta Q = -\alpha A \left[\frac{\partial T}{\partial x} + \frac{\partial}{\partial x} \left(\frac{\partial T}{\partial x} \right) \Delta x \right] \Delta t \tag{2}$$

Supposedly, the heat input into the sample is W per volume unit, and the loss due to irradiation and convection is neglected.

Therefore, the energy obtained in per length at Δx is

$$\Delta Q + W A \Delta x \Delta t = \alpha A \frac{\partial^2 T}{\partial x^2} \Delta x \Delta t \tag{3}$$

Consequently, the rate of temperature variation is

$$\frac{\partial T}{\partial x} = \frac{1}{\rho c} \left(W + \alpha \frac{\partial^2 T}{\partial x^2} \right) \tag{4}$$

where ρ is the density of sample and c is the specific heat capacity.

When the processing is stable, $\frac{\partial T}{\partial x} = 0$, then

$$W = -\alpha \frac{\partial^2 T}{\partial x^2} \tag{5}$$

After integration,

$$\frac{\partial T}{\partial x} = -\frac{W}{\alpha} x + b \tag{6}$$

When $x = \frac{1}{2} L$, $\frac{\partial T}{\partial x} = 0$, it obtains

$$b = \frac{WL}{2\alpha} \tag{7}$$

Integratedly, then

$$T = -\frac{W}{2\alpha}x^2 + \frac{WL}{2\alpha}x + b' \tag{8}$$

At $x = 0$ and $T = T_0$, so $b' = T_0$; therefore,

$$T = -\frac{W}{2\alpha}x^2 + \frac{WL}{2\alpha}x + T_0 \tag{9}$$

or

$$T - T_0 = \frac{W}{2\alpha}(L - x)x \tag{10}$$

At $x = \frac{1}{2}L$ and $T = T_{max}$, so

$$T_{max} - T_0 = \frac{WL^2}{8\alpha} \tag{11}$$

Assumption: $T = T_{max} - \Delta T$, then

$$T_{max} - \Delta T - T_0 = 4\frac{(T_{max} - T_0)}{L^2}(L - x)x \tag{12}$$

Therefore,

$$x = \frac{L}{2}\left[1 \pm \sqrt{\frac{\Delta T}{T_{max} - T_0}}\right] \tag{13}$$

As a result, the length between T_{max} and $T_{max} - \Delta T$ is

$$\Delta x = L\sqrt{\frac{\Delta T}{T_{max} - T_0}} \tag{14}$$

According to Eq. (14), it reveals that with the increment of temperature difference, the area between the solid phase and liquid phase increases simultaneously. However, if the temperature is too high, it will make the welding failure because the area between the solid phase and liquid phase enlarges. As a result, when the samples are impacted, the relative sliding of samples occur [21–23]. Meanwhile, the grain size and microstructure of AMCs will be too larger and coarser to decrease the property of the welded joints.

Furthermore, considering the practical situations during the welding process, the resistance between the two welded pieces due to the heterogeneous materials at the welding area is definitely higher than that of the calculation on the basis of the theory. Consequently, Eq. (14) will be

$$\Delta x = \eta L\sqrt{\frac{\Delta T}{T_{max} - T_0}} \tag{15}$$

where η is the coefficient of the influence of hetero-resistance at the welding area.

## 3.2. Microstructure of welded joint at various temperatures

The fractographs of SiC$_p$/A356 are shown in **Figure 4**. It illustrates that when the welding temperature is 563°C, the initial morphology of substrate is still obviously detected, and some sporadic welded locations appear together with some rather densely scattering bare reinforcement particles as shown in **Figure 4a**. With the welding temperature increasing to 565°C, more liquid phases form. Under the effect of pulse-impact, some wet locations in the
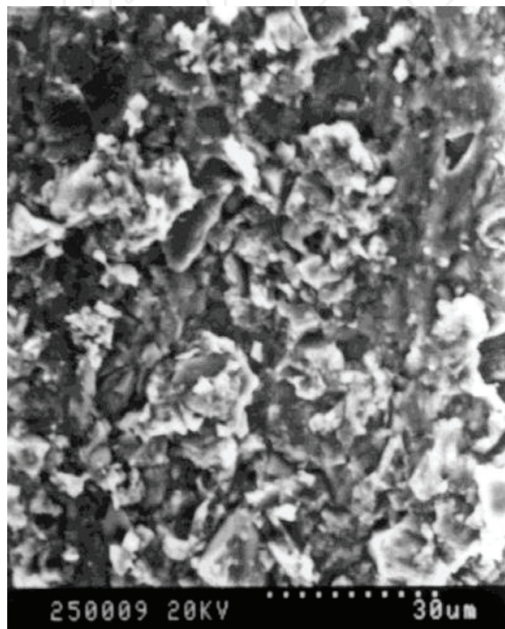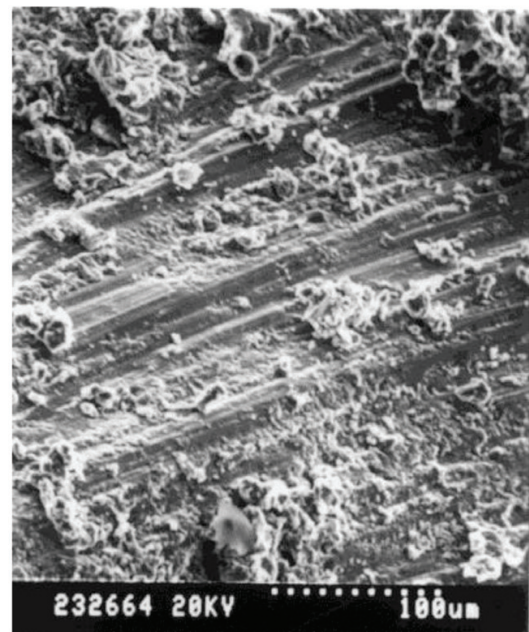

(a) 563 °C
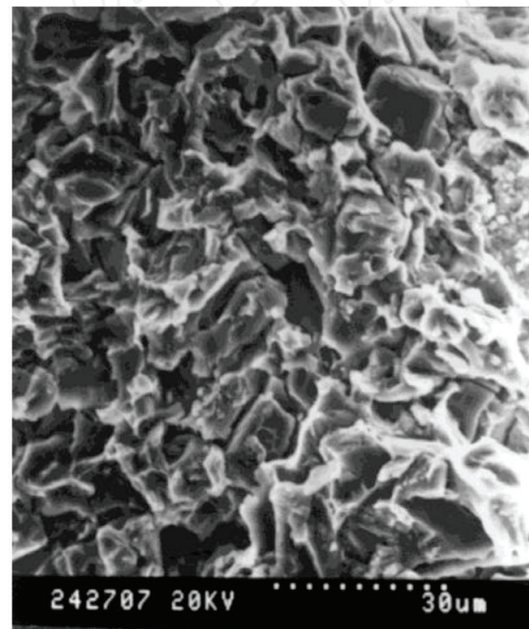
(b) 565 °C
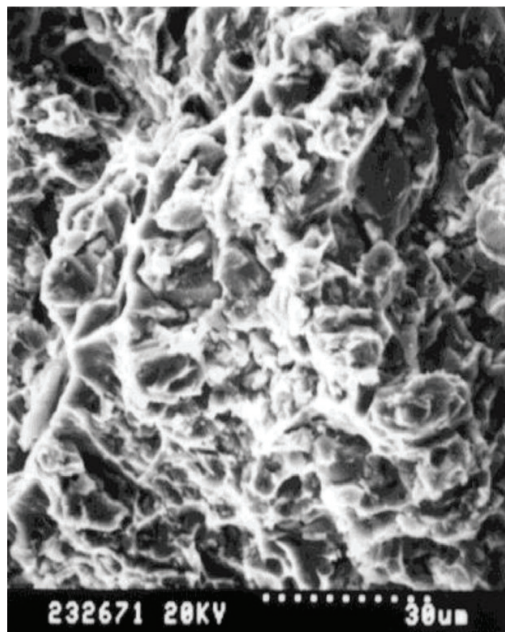
(c) 570 °C

(d) 575 °C

Figure 4. Fractographs of SiC$_p$/A356 at various temperatures. (a) 563°C, (b) 565°C, (c) 570°C and (d) 575°C.

joint excellently weld, and the condition of the aggregated solid reinforcement particles is improved. However, the bare reinforcement particles still distribute on the fractographic surface. It indicates that substrates do not weld ideally and it consequently results in a low-strength joint (**Figure 4b**).

Figure 4c shows the fractograph of welded joint at 570°C. It illustrates that the fracture is dimple fracture. Moreover, SEM image of the fracture surface shows some reinforcement particles (SiC) in the dimple. In order to confirm the state of these reinforcement particles, particles itself and matrix near to these particles were analyzed by energy-dispersive X-ray analysis (EDX). The result is expressed in **Figure 5**. It indicates that reinforcement particles (SiC) are wet by matrix alloy successfully suggesting that the reinforcement particles have been perfectly wet and the composite structure of reinforcement/reinforcement has been changed to the state of reinforcement/matrix /reinforcement.

As welding temperature increases to 575°C, it leads to more and more liquid-phase matrix alloy distributed in the welded interface. Meanwhile, more liquid-phase matrix alloy reduces the effect of impact on the interface of the welded joints; subsequently, the application of transient pulse-impact causes the relative sliding of the weldpieces that jeopardizes ultimately the formation of proper joint as shown in **Figure 4d**.

The relevant fractographies of SiC_p/6061Al and Al_2O_{3p}/6061Al at various welding temperatures are shown from **Figures 6** to **7**. It shows that the fracture surfaces under the effect of pulse-impact are similar to that of SiC_p/A356. The fractures are all dimple fractures with some reinforcement particles (SiC, Al_2O_3) in the dimple.

SEM results of the fracture surface show that the reinforcement particles have been perfectly wet and the composite structure of reinforcement/reinforcement has been changed to the state of reinforcement/matrix /reinforcement. XRD pattern of the fracture surfaces (**Figure 8**) does not show the existence of any harmful phase or brittle phase of Al_4C_3. This suggests the effective interface transfers between reinforcement particles and matrix in the welded joint that subsequently provides favorable welding strength [16–18].

3.3. Effect of pulse-impact on SiCp/6061Al LPPIDW on the interface reaction

During LPPIDW, SiC_p/6061Al welding temperature is so high that the reaction between SiC particles and aluminum matrix occurs as follows:

$$3SiC(s) + 4Al(l) \rightarrow Al_4C_3(s) + 3Si(s) \tag{16}$$

The relevant free energy [24] is

$$\Delta G(\text{J} \cdot \text{mol}^{-1}) = 113900 - 12.06T\ln T + 8.92 \times 10^{-3}T^2 + 7.53 \times 10^{-4}T^{-1} + 21.5T + 3RT\ln \alpha_{[Si]} \tag{17}$$

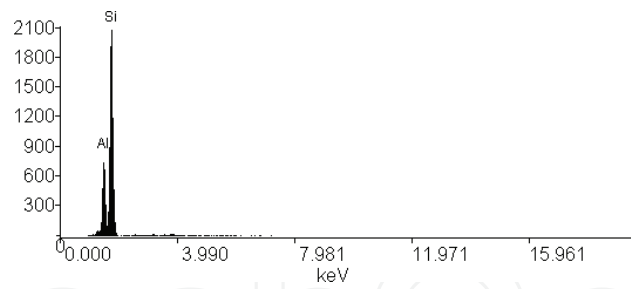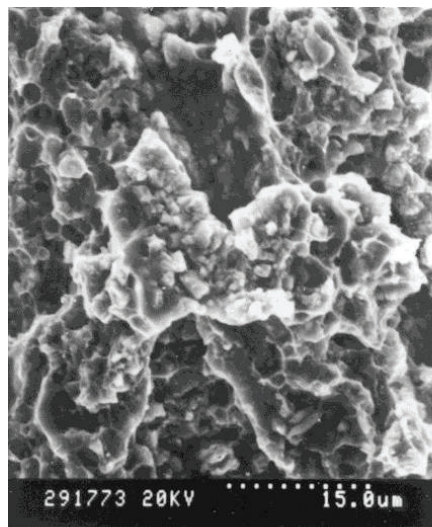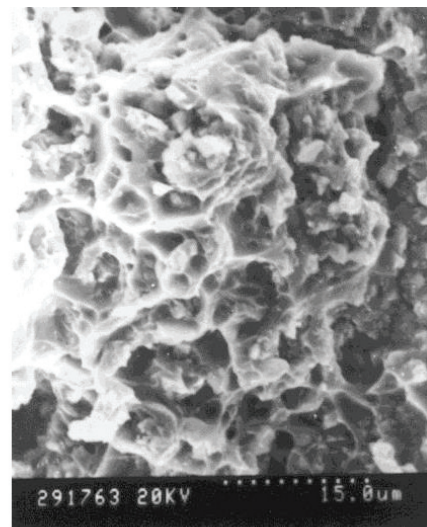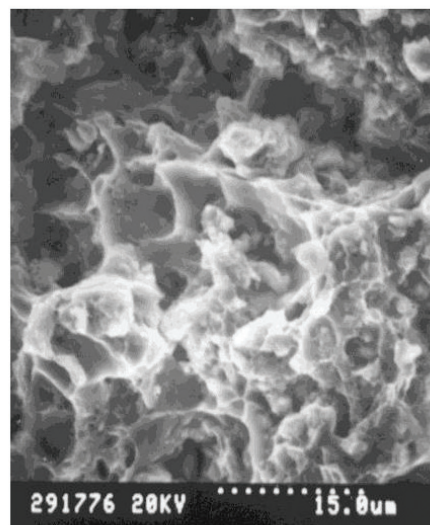where $\alpha_{[Si]}$ Si is the activity in the liquid of aluminum.

Figure 5. Energy-dispersive X-ray analysis of the fracture surface of SiC$_P$/A356.

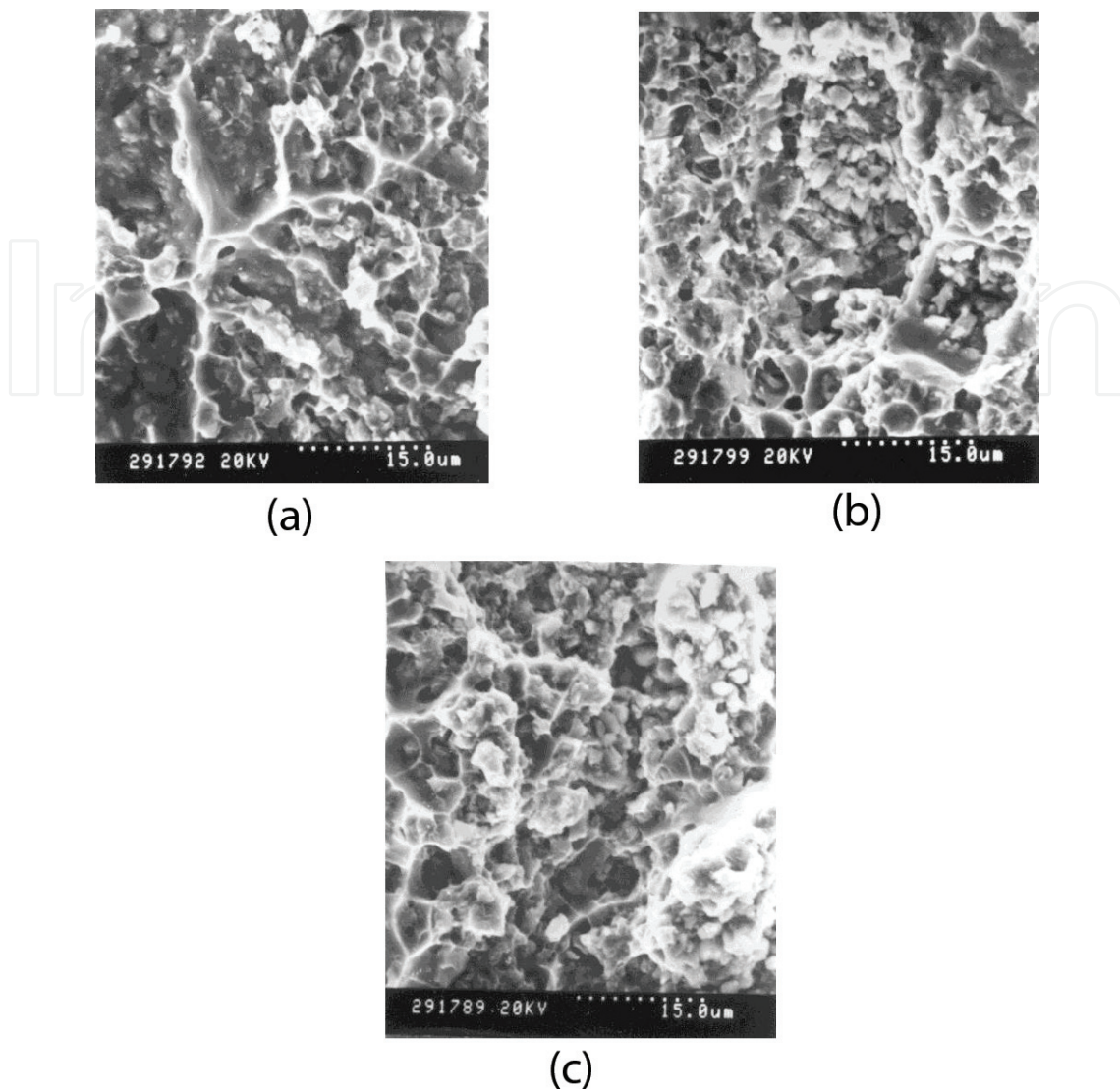**Figure 6.** Fractographs of SiC$_P$/6061Al at various temperatures. (a) 620°C, (b) 623°C and (c) 625°C.

Figure 7. Fractographs of $Al_2O_{3p}/6061Al$ at various temperatures. (a) 641°C, (b) 644°C and (c) 647°C.

In the viewpoint of thermodynamics, $\Delta G > 0$ during LPPIDW $SiC_p/6061Al$. Therefore, the reaction of Eq. (16) does not occur. However, in accordance with binary alloy-phase diagrams of Al-Si as shown in **Figure 9** [11], Si will dissolve in the aluminum matrix during the welding, and the activity of Si in the liquid aluminum varies at various temperatures. The relationship between free energy and welding temperature in the interface after considering Si dissolution in the aluminum matrix is shown in **Figure 10**, which indicts that Eq. (16) will occur in the welding.

It is well known that the interfaces between the reinforcement (particles) and matrix are playing the extremely vital role in AMCs, especially in adjusting their matches. The slight reaction at the interfaces is propitious to improve the property of welded joints due to the release of internal stress, which is caused by the hetero-matches between the
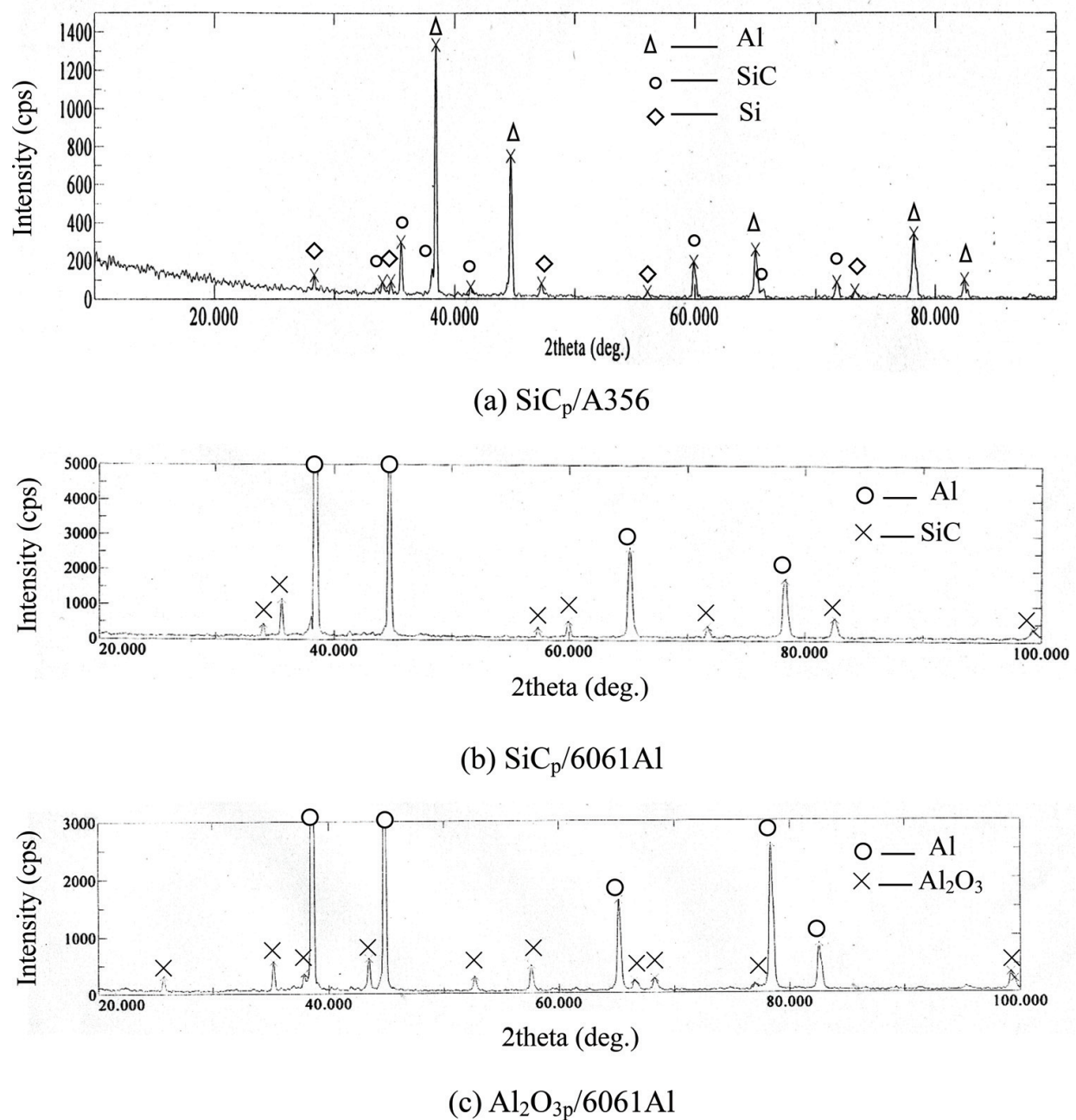
Figure 8. XRD pattern of the fracture surfaces. (a) SiC$_p$/A356, (b) SiC$_p$/6061Al and (c) Al$_2$O$_{3p}$/6061Al.

reinforcements and matrix. The distribution of dislocations at the interface is shown in **Figure 11**. It illustrates that the density of dislocations decreases remarkably, especially compared with that of its nearing area, which elucidates that the effective reaction at the interface occurs and releases the internal stress due to the hetero-matches between the reinforcement/particle (SiC) and matrix. Consequently, the property of welded joints improves compellingly and convincingly.
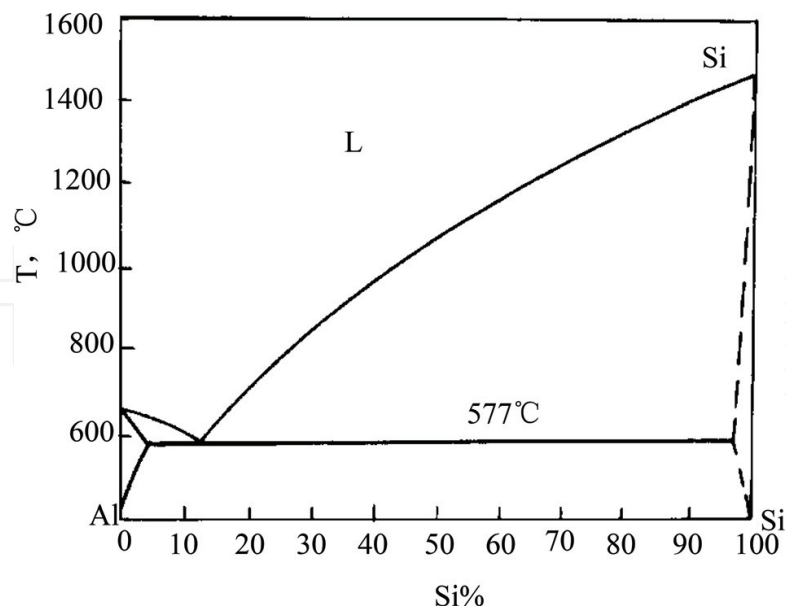
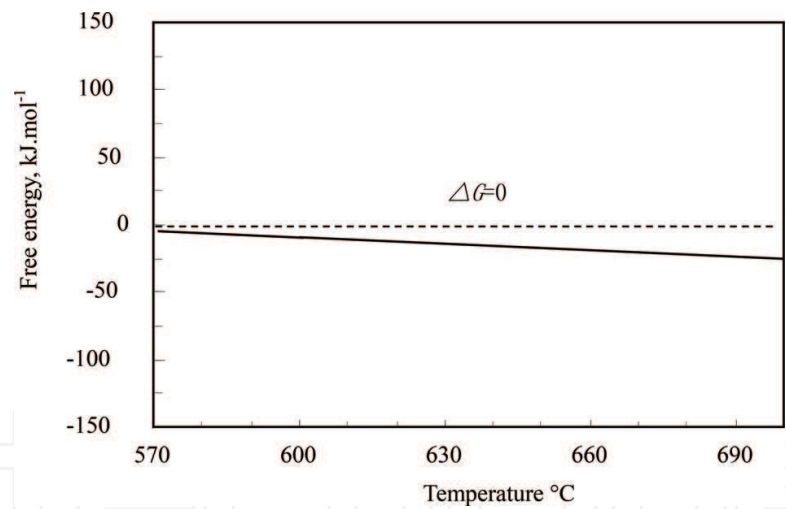**Figure 9.** Binary alloy phase diagrams of al-Si [25].

Figure 10. Relationship between free energy and welding temperature in the interface.

Also, the results shown in **Figure 6** of $SiC_p/6061Al$ are better than that of $Al_2O_{3p}/6061Al$ shown in **Figure 7** just due to this interfacial reaction between the reinforcement and matrix, which releases the thermal mismatch stress to an acceptable extent between the reinforcement and matrix to allow load transfer from the matrix to reinforcement successfully. As a result, it has advantageous effect of improving the strength of welded joints further [18].

Figure 11. Distribution of dislocations at the interface.

4. Conclusion

The fractography results of liquid-phase-pulse-impact diffusion welding of particle rein-forcement aluminum matrix composites (SiC$_p$/A356, SiC$_p$/6061Al, and Al$_2$O$_{3p}$/6061Al) show that:

(1) The area of the solid-phase and liquid-phase coexistence in the welding can be calculated by $\Delta x = \eta L \sqrt{\frac{\Delta T}{T_{max} - T_0}}$

(2) The fracture of welded joints with optimal processing parameters is the dimple fracture with some reinforcement particles (SiC, Al$_2$O$_3$) in the dimples.

(3) Distinctly clear interface between reinforcement particle and matrix overcomes some diffu-sion problems normally encountered in conventional diffusion welding and prevents the formation of harmful microstructure or brittle phase in the welded joint.

(4) The slight reaction occurs at the interfaces of SiC$_p$/6061Al, which is propitious to improve the property of welded joints because of the release of internal stress caused by the hetero-matches between the reinforcements and matrix.

Author details

Kelvii Wei Guo[1,2*]

*Address all correspondence to: guoweichinese@yahoo.com

1 State Key Laboratory of Millimeter Waves (Partner Laboratory in City University of Hong Kong), City University of Hong Kong, Kowloon Tong, Kowloon, Hong Kong

2 Department of Mechanical and Biomedical Engineering, City University of Hong Kong, Kowloon Tong, Kowloon, Hong Kong

References

[1] Nair SV, Tien JK, Bates RC. SiC-reinforced aluminium metal matrix composites. International Metals Reviews. 1995;**30**(6):275-288

[2] Avettand-Fènoël MN, Simar AA. Review about friction stir welding of metal matrix composites. Materials Characterization. 2016;**120**:1-17

[3] Pandey U, Purohit R, Agarwal P, Dhakad SK, Rana RS. Effect of TiC particles on the mechanical properties of aluminium alloy metal matrix composites (MMCs). Materials Today: Proceedings Part D. 2017;**4**(4):5452-5460

[4] Butt J, Mebrahtu H, Shirvani H. Microstructure and mechanical properties of dissimilar pure copper foil/1050 aluminium composites made with composite metal foil manufacturing. Journal of Materials Processing Technology. 2016;**238**:96-107

[5] Loyd DJ. Particle reinforced aluminum magnesium composites. International Materials Reviews. 1994;**39**(1):1-22

[6] Rana RS, Purohit R, Soni VK, Das S. Characterization of mechanical properties and microstructure of Aluminium alloy-SiC composites. Materials Today: Proceedings. 2015;**2**(4–5):1149-1156

[7] Pirondi A, Collini L. Analysis of crack propagation resistance of Al-Al$_2$O$_3$ particulate-reinforced composite friction stir welded butt joints. International Journal of Fatigue. 2009;**31**(1):111-121

[8] Rotundo F, Ceschini L, Morri A, Jun TS, Korsunsky AM. Mechanical and microstructural characterization of 2124Al/25vol.%SiCp joints obtained by linear friction welding (LFW). Composite Part A: Applied Science and Manufacturing. 2010;**41**(9):1028-1037

[9] Gómez de Salazar JM, Barrena MI. Dissimilar fusion welding of AA7020/MMC reinforced with Al$_2$O$_3$ particles. Microstructure and mechanical properties. Materials Science and Engineering A. 2003;**352**:162-168

[10] Bataev IA, Lazurenko DV, Tanaka S, Hokamoto K, Bataev AA, Guo Y, Jorge Jr. AM. High cooling rates and metastable phases at the interfaces of explosively welded materials. Acta Materialia 2017;**135**: 277–289.

[11] Maity J, Pal TK, Maiti R. Transient liquid phase diffusion bonding of 6061-15 wt% SiCp in argon environment. Journal of Materials Processing Technology. 2009;**209**(7): 3568-3580

[12] Schell JSU, Guilleminot J, Binetruy C, Krawczak P. Computational and experimental analysis of fusion bonding in thermoplastic composites: Influence of process parameters. Journal of Materials Processing Technology. 2009;**209**(11):5211-5219

[13] Sundaram NS, Murugan N. Tensile behavior of dissimilar friction stir welded joints of aluminum alloys. Materials & Design. 2010;**31**(9):4184-4193

[14] Arik H, Aydin M, Kurt A, Turker M. Weldability of Al_4C_3-Al composites via diffusion welding technique. Materials & Design. 2005;**26**(6):555-560

[15] American Welding Society. Welding Handbook Miami: American Welding Society; 1996.

[16] Chamanfar A, Pasang T, Ventura A, Misiolek WZ. Mechanical properties and microstructure of laser welded Ti-6Al-2Sn-4Zr-2Mo (Ti6242) titanium alloy. Materials Science and Engineering: A. 2016;**663**:213-224

[17] Wert JA. Microstructures of friction stir weld joints between an Aluminium-Base metal matrix composite and a monolithic Aluminium alloy. Scripta Materialia. 2003;**49**(6):607-612

[18] Fernandez GJ, Murr LE. Characterization of tool wear and weld optimization in the friction-stir welding of cast aluminum 359+20% SiC metal-matrix composite. Materials Characterization. 2004;**52**(1):65-75

[19] Hsu CJ, Kao PK, Ho NJ. Ultrafine-grained al–Al_2Cu composite produced in-situ by friction stir processing. Scripta Materialia. 2005;**53**(3):341-345

[20] Marzoli LM, Strombeck AV, Dos Santos JF, Gambaro C, Volpone LM. Friction stir welding of an AA6061/Al_2O_3/20p reinforced alloy. Composites Science and Technology. 2006;**66**(2):363-371

[21] Guo W, Hua M, Ho JKL. Study on liquid-phase-impact diffusion welding SiC_p/ZL101. Composites Science and Technology. 2007;**67**(6):1041-1046

[22] Guo W, Hua M, Ho JKL, Law HW. Mechanism and influence of pulse-impact on properties of liquid phase pulse-impact diffusion welded SiCp/A356. The. International Journal of Advanced Manufacturing Technology. 2009;**40**(9–10):898-906

[23] Guo W, Hua M, Law HW, Ho JKL. Liquid phase impact diffusion welding of SiC_p/6061Al and its mechanism. Materials Science and Engineering: A. 2008;**490**(1–2):427-437

[24] Isekl T, Kameda T, Maruyama T. Interfacial reaction between SiC and aluminum during joining. Journal of Materials Science. 1984;**19**:1692-1698

[25] Ohring M. Engineering Materials Science. San Diego: Academic Press; 1995